

Identification of Substituted 3-[(4,5,6,7-Tetrahydro-1*H*-indol-2-yl)methylene]-1,3-dihydroindol-2-ones as Growth Factor Receptor Inhibitors for VEGF-R2 (Flk-1/KDR), FGF-R1, and PDGF-R β Tyrosine Kinases

Li Sun,^{*,§} Ngoc Tran,[§] Congxing Liang,[§] Steve Hubbard,[‡] Flora Tang,[§] Kenneth Lipson,[§] Randall Schreck,[§] Yong Zhou,[§] Gerald McMahon,[§] and Cho Tang^{§,*}

SUGEN, Inc., 230 East Grand Avenue, South San Francisco, California 94080-4811, and Skirball Institute of Biomolecular Medicine and Department of Pharmacology, New York University Medical Center, New York, New York 10016

Received December 15, 1999

A series of new 3-substituted indolin-2-ones containing a tetrahydroindole moiety was developed as specific inhibitors of receptor tyrosine kinases associated with VEGF-R, FGF-R, and PDGF-R growth factor receptors. These compounds were evaluated for their inhibitory properties toward VEGF-R2 (Flk-1/KDR), FGF-R1, PDGF-R β , p60^{c-Src}, and EGF-R tyrosine kinases and their ability to inhibit growth factor-dependent cell proliferation. Structure–activity relationships of this new pharmacophore have been determined at the level of kinase inhibition. Compounds containing a propionic acid moiety at the C-3' position of the tetrahydroindole ring represented the most potent indolin-2-ones to inactivate the VEGF, FGF, and PDGF receptor kinases. The inhibitory activities of **9d** against VEGF-R2 (Flk-1), **9h** against FGF-R1, and **9b** against PDGF-R β were 4, 80, and 4 nM, respectively. However, all of these compounds were inactive when tested against the EGF-R tyrosine kinase. Compounds **9a** and **9b** represented the most potent inhibitors of these classes to inhibit both biochemical kinase and growth factor-dependent cell proliferation for these three targets. In addition, compound **9a** was cocrystallized with the catalytic domain of FGF-R1 providing evidence to explain the structure–activity relationship results. This study has provided evidence to support the potential of these new tyrosine kinase inhibitors for the treatment of angiogenesis and other growth factor-related diseases including human cancers.

Introduction

It is well-accepted that de novo angiogenesis is critical to the growth of solid tumors.¹ In this regard, newly formed capillaries around the tumor mass have been suggested to (1) provide nutrients and growth factors for rapid tumor growth, (2) remove waste generated by tumor metabolism, and (3) transport tumor cells to locations far from the primary site to cause tumor metastasis. Because of these implications, it is not surprising that novel treatments to inhibit tumor angiogenesis have become a means to develop new cancer therapies. In this regard, large numbers of cellular components, including growth factors and cytokines, have been implicated in the tumor angiogenic process.² One key growth factor is VEGF (vascular endothelial growth factor) and its cognate receptor tyrosine kinases (VEGF-R2 (Flk-1) and VEGF-R1 (Flt-1)). VEGF and its receptors have been shown to play direct role in tumor angiogenesis by promoting endothelial cell proliferation and vascular permeability, key processes in angiogenesis. Importantly, VEGF-R2 (Flk-1) has been shown to be expressed selectively in endothelial cells.³

In addition, other studies have demonstrated that other growth factors and their cognate receptor tyrosine

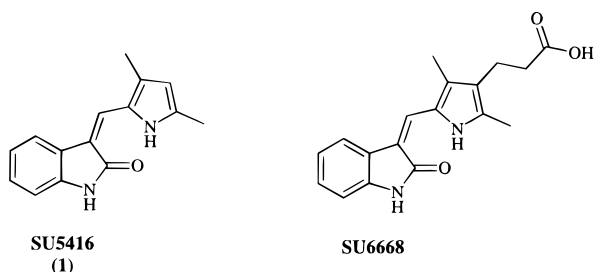
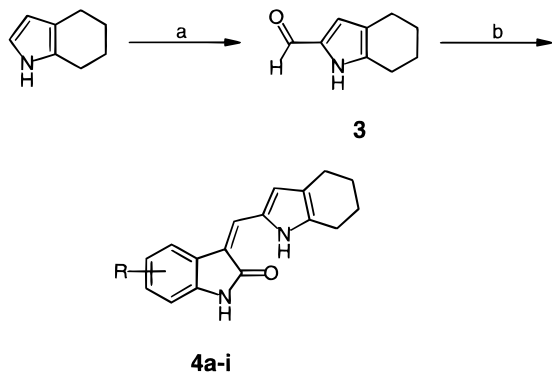
kinases (RTKs) such as FGF (fibroblast growth factor) and PDGF (platelet-derived growth factor) may play a direct or indirect role in the tumor angiogenic process. For instance, FGF was found to be a mitogen of different cell types including vascular endothelial cells and fibroblasts and, in some cases, may induce the expression of VEGF.⁴ Studies using in vitro angiogenesis assays have indicated that both VEGF and FGF may cooperate during new blood vessel development.⁵ In contrast, PDGF has been shown to stimulate the growth of pericytes and fibroblast-like cells which have been shown to be required for the formation of the capillaries during angiogenesis. Additionally, PDGF has been shown to play a role in angiogenesis leading to upregulation of VEGF expression.⁴ Furthermore, both FGF and PDGF may be involved in a hypothesized “angiogenic switch” following VEGF signaling during early stages of tumor growth.⁶

Recently, diverse pharmacophores of small molecule inhibitors have been emerged as antiangiogenic agents targeting at different RTKs including the VEGF and FGF receptors.⁷ Our own previous studies have demonstrated the potential of 3-substituted indolin-2-ones as antiangiogenic agents.^{8,9} As shown in Chart 1, two compounds (SU5416, **1**, and SU6668) from the indolin-2-one pharmacophore have advanced into clinical trials.^{10,11} The goal of this present study was to further diversify the indolin-2-one pharmacophore in order to develop catalytic kinase inhibitors that could block

* To whom correspondence should be addressed. Phone: (650)553-8480. Fax: (650)553-8348. E-mail: connie-sun@sugen.com.

[§] SUGEN, Inc.

[‡] New York University Medical Center.

Chart 1. Indolin-2-ones in Clinical Trials**Scheme 1.** Synthesis of Substituted 3-[(4,5,6,7-Tetrahydro-1*H*-indol-2-yl)methylene]-1,3-dihydroindol-2-ones **4a–i**^a

^a (a) POCl₃, ClCH₂CH₂Cl, 40 °C, 4 h; (b) substituted indolin-2-ones, piperidine, ethanol, reflux, 2–4 h.

signal transduction pathways associated with VEGF, FGF, and PDGF growth factor receptors. These three receptor types belong to a large family of tyrosine kinases denoted as “split” kinases due to the presence of a unique insert region in the catalytic domain. Two classes of substituted indolin-2-ones containing a tetrahydroindole moiety at the C-3 position of the indolin-2-one core were designed and evaluated for their potential to inhibit kinase activities (Tables 1 and 2). Data related to biochemical kinase activity, cocrystallography of a prototype compound in the FGF-R1 catalytic domain, and antiproliferative activities for growth factors are shown and discussed.

Chemistry

The compounds in this report were prepared by aldolcondensation of the substituted indolin-2-ones and corresponding aldehydes in the presence of base in ethanol as described previously.^{8,9} The two aldehydes used in this study were prepared as follows.

Tetrahydroindole-2-carboxaldehyde (**3**) (Scheme 1) was prepared via a Vilsmeier formylation reaction of commercially available tetrahydroindole (Scheme 1). Condensation of this aldehyde with substituted indolin-2-ones gave the corresponding **4a–i** (Scheme 1 and Table 1).

Compounds **9a–i** were synthesized by condensing substituted indolin-2-ones with 3-(2-carboxyethyl)-4,5,6,7-tetrahydroindole-2-carboxaldehyde (compound **8** in Scheme 2). Compound **8** was prepared starting from the 4-cyclohex-1-enylmorpholine which was acylated with 3-chlorocarbonylpropionic acid ethyl ester to give 4-(2-morpholin-4-ylcyclohex-1-enyl)-4-oxobutyric acid ethyl ester (compound **5** in Scheme 2). Compound **5** was

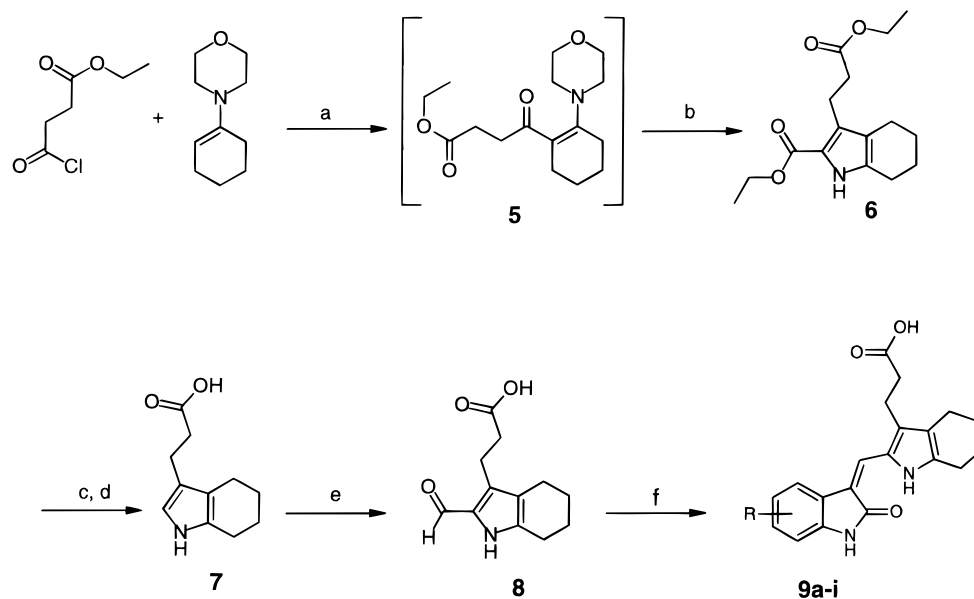
then condensed with diethyl aminomalonate hydrochloride to give 3-(2-ethoxycarbonyl-ethyl)-4,5,6,7-tetrahydro-1*H*-indole-2-carboxylic acid ethyl ester (compound **6** in Scheme 2). Hydrolysis of **6** followed by decarboxylation resulted in compound **7** that upon formylation gave **8**.

All of the compounds prepared in this report exist in the *Z* (*cis*) conformation due to the intramolecular hydrogen bonding between the NH-1' of the tetrahydroindole ring and the carbonyl group at the C-2 position of the indolin-2-one core as we described previously.⁸

Results and Discussion

Compounds were evaluated for their inhibitory activity toward tyrosine phosphorylation for the VEGF-R2 (Flk-1), FGF-R1, PDGF-Rβ, p60^{c-Src}, and EGF-R tyrosine kinases. The p60^{c-Src} kinase has been shown to be activated by a wide variety of RTKs following growth factor addition.¹³ It was of importance to include an analysis of kinase inhibition for p60^{c-Src} in order to fully interpret results using growth factor-stimulated proliferation in cells since inhibitors of p60^{c-Src} may score as inhibitors of all proliferation assays where this kinase may be activated. These data would aid in our understanding of the effects of the compound on RTKs or downstream events. Biochemical tyrosine autophosphorylation assays were used to assess the inhibitory potency of all compounds toward PDGF-Rβ and EGF-R tyrosine kinases, respectively, whereas peptide-based transphosphorylation assays were performed for VEGF-R2 (Flk-1), FGF-R1, and p60^{c-Src} kinase activities. In addition, these compounds were also evaluated in growth factor-stimulated cell proliferation assays using either human umbilical vein endothelial cells (HUVECs) or NIH3T3 mouse fibroblast cells. IC₅₀ values were defined as the concentration of a compound required to achieve 50% inhibition of maximal tyrosine autophosphorylation, transphosphorylation, or growth factor-stimulated growth as measured by bromodeoxyuridine (BrdU) incorporation when compared to vehicle-treated controls (DMSO). The results for these compounds are summarized in Tables 1 and 2. The structure–activity relationships (SAR) are discussed separately for these two classes of compounds.

A. Substituted 3-[(4,5,6,7-Tetrahydroindol-2-yl)methylidene]indolin-2-ones. In our effort to diversify substitutions on the pyrrole ring at the C-3 position of the indolin-2-one core, 3-[(4,5,6,7-tetrahydroindol-2-yl)methylidene]indolin-2-ones (**4a** analogues in Table 1) were synthesized and showed interesting biological properties. By comparison to **1**, **4a** showed a similar kinase profile to **1** when tested against VEGF-R2 (Flk-1) and FGF-R1 and was found to be a slightly more potent than **1** when tested against PDGF-Rβ (IC₅₀ = 5.46 μM for **4a** vs IC₅₀ = 10.1 μM for **1**) (Table 1). Of particular interest, **4a** was 4-fold more potent than **1** when tested against the p60^{c-Src} kinase. Computational studies based in part on previous cocrystallographic studies suggested that this might be the result of a favorable interaction of the tetrahydroindole moiety with hydrophobic valine present in the adenine binding pocket of p60^{c-Src} kinase.¹² On the other hand, corre-

Scheme 2. Synthesis of Substituted 3-[2-(2-Oxo-1,2-dihydroindol-3-ylidenemethyl)-4,5,6,7-tetrahydro-1*H*-indol-3-yl]propionic Acids **9a–i**^a

^a (a) $(\text{C}_2\text{H}_5)_3\text{N}$, $\text{ClCH}_2\text{CH}_2\text{Cl}$, reflux, 30 min; (b) diethyl aminomalonate hydrochloride, sodium acetate, acetic acid, reflux, 2 h; (c) NaOH , reflux, 1.5 h; (d) $\text{HCl}(\text{aq})$; (e) POCl_3 , DMF , $\text{ClCH}_2\text{CH}_2\text{Cl}$; (f) substituted indolin-2-ones, piperidine, ethanol, reflux, 4 h.

Table 1. Inhibition of Tyrosine Kinase Activities and Growth Factor-Dependent Cell Proliferation Using Compounds **4a–i**

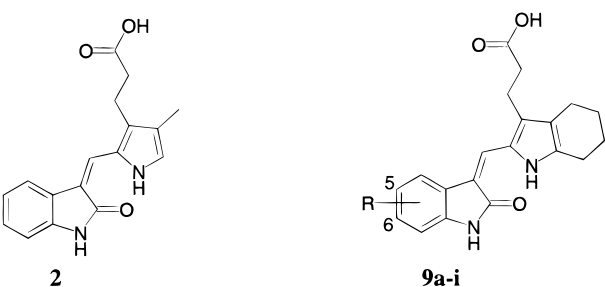
no.	compounds R	inhibition of tyrosine kinase activity (IC_{50} , μM) ^a					inhibition of cell proliferation (IC_{50} , μM) ^a			
		VEGF-R2	FGF-R1	PDGF-R β	p60 ^{c-Src}	EGF-R	VEGF	FGF	PDGF	EGF
1		0.70	7.08	10.1	16.4	>100	0.04	50.0	4.54	>50
4a	H	0.48	10.5	5.46	4.74	>100	0.07	>50	3.22	>50
4b	5-Br	0.07	13.3	0.92	4.92	>100	0.11	24.6	2.01	>50
4c	5-SO ₂ NH ₂	0.03	0.22	11.5	0.08	>100	0.65	2.38	0.24	6.00
4d	5-COOH	0.02	0.31	1.03	0.12	>100	0.03	2.80	9.98	>50
4e	6-OCH ₃	12.1	>20	3.46	>20	>100	>50	>50	1.08	>50
4f	6-phenyl	>20	>20	70.6	>20	>100	>12.5	>12.5	>50	>50
4g	6-(3-OCH ₃ phenyl)	>20	17.5	>100	>20	>100	>50	>50	>50	>50
4h	6-(2-OCH ₃ phenyl)	20	17.7	13.9	>20	>100	13.0	14.64	1.40	34.08
4i	6-(4-OCH ₃ phenyl)	>20	>20	94.01	>20	>100	>12.5	>12.5	>50	>50

^a IC_{50} values were determined by at least two separate tests and are reported as mean values.

sponding amino acids in VEGF-R2 (Flk-1), FGF-R1, and PDGF-R β are hydrophilic lysine, lysine, and arginine residues, respectively. These several features may help explain, in part, the improved inhibitory activity of the tetrahydroindole-containing indolin-2-one series toward p60^{c-Src} kinase as compared to VEGF-R2 (Flk-1), FGF-R1, and PDGF-R β . In addition, bromination at the C-5 position of the **4a** core resulted in retaining the potencies against both FGF-R1 and p60^{c-Src} and resulted in a 7- and 6-fold increase in potency (**4b**) toward VEGF-R2 (Flk-1) and PDGF-R β , respectively. This suggested that small lipophilic substituents at the C-5 position on the indolin-2-one core might favor inhibitory activities for these targets. Both **4a** and **4b** were found to be selective inhibitors for VEGF-R2 (Flk-1).

Hydrophilic substituents at the C-5 position of **4c** (aminosulfonyl) and **4d** (carboxylic acid) greatly improved the potencies toward both VEGF-R2 (Flk-1) and

FGF-R1 kinases. Both of these compounds were found to be the most potent inhibitors of VEGF-R2 (Flk-1) and FGF-R1 in this series. This result is in accordance with our previous studies indicating that hydrophilic substitutions (carboxylic acid and aminosulfonyl) at the C-5 position of the indolin-2-one core could enhance the inhibitory potency against both VEGF-R2 (Flk-1) and FGF-R1 kinase.⁹ Interestingly, compounds **4c** and **4d** were also found to be highly potent toward p60^{c-Src} kinase with IC_{50} values of 0.08 and 0.12 μM , respectively, compared to the IC_{50} value of 4.74 μM for **4a** (Table 1). Compound **4c** represented one of the most potent inhibitors of p60^{c-Src} kinase in this study. The respective crystallographic structures of FGF-R1¹² and p60^{c-Src} have indicated that although amino acids in the phosphate binding region were conserved, residues Asn391 and Asp404 in p60^{c-Src} protrude significantly more into the ATP binding site than those found in

Table 2. Inhibition of Tyrosine Kinase Activities and Growth Factor-Dependent Cell Proliferation Using Compounds **9a–i**


compounds		inhibition of tyrosine kinase activity (IC ₅₀ , μM) ^a					inhibition of cell proliferation (IC ₅₀ , μM) ^b			
no.	R	VEGF-R2	FGF-R1	PDGF-Rβ	p60 ^{c-Src}	EGF-R	VEGF	FGF	PDGF	EGF
2		0.02	0.03	0.51	10.6	>100	0.05	2.80	28.4	>50
9a	H	0.09	0.27	0.24	1.89	>100	0.002	0.01	7.66	>50
9b	5-Br	0.03	0.27	0.004	1.27	>100	0.0003	0.10	1.38	>50
9c	5-SO ₂ NH ₂	0.60	0.20	<0.78	0.68	29.1	16.5	29.0	>50	>50
9d	5-COOH	0.004	0.22	0.02	0.06	56.5	4.49	>25	>50	>50
9e	6-OCH ₃	0.38	1.08	19.3	1.39	>100	0.02	1.60	3.01	>50
9f	6-phenyl	0.05	1.27	0.04	0.11	>100	0.09	3.80	0.92	31.6
9g	6-(3-OCH ₃ phenyl)	0.07	1.35	0.68	0.10	8.88	0.06	0.18	1.36	37.2
9h	6-(2-OCH ₃ phenyl)	0.06	0.08	0.87	0.84	>100	2.70	6.91	1.28	41.5
9i	6-(4-OCH ₃ phenyl)	0.03	0.88	5.43	0.06	>100	0.18	0.53	1.32	37.8

^a IC₅₀ values for VEGF-R2 (Flk-1) and FGF-R1 were determined by at least two separate tests and are reported as mean values. ^b IC₅₀ values were determined by at least two separate tests and are reported as mean values.

Table 3. Data Collection and Refinement Statistics

Data Collection					
resolution (Å)	observations (<i>N</i>)	completeness (%)	redundancy	<i>R</i> _{sym} ^a (%)	signal ⟨ <i>I</i> /σ <i>I</i> ⟩
30.0–2.2	69057	98.2 (96.3) ^b	1.9	3.8 (19.7) ^b	12.4
Refinement ^c					
resolution deviations (Å)	reflections (<i>N</i>)	<i>R</i> _{cryst} ^d (%)	root-mean-square		
25.0–2.2	33894	22.1 (26.5) ^f	bonds (Å)	angles (deg)	<i>B</i> -factors ^e (Å ²)
			0.006	1.2	1.1

^a $R_{\text{sym}} = 100 \times \sum_{hkl} \sum_i |I_i(hkl) - \langle I(hkl) \rangle| / \sum_{hkl} \sum_i I_i(hkl)$. Data are from one crystal. ^b Value in parentheses is for the highest resolution shell. ^c Atomic model includes 550 residues (two kinase molecules), two **9a** molecules, and 223 water molecules (4631 atoms). ^d $R_{\text{cryst}} = 100 \times \sum_{hkl} (|F_o(hkl)| - |F_c(hkl)|) / \sum_{hkl} |F_o(hkl)|$, where F_o and F_c are the observed and calculated structure factors, respectively ($F_o > 2\sigma$). ^e For bonded protein atoms. ^f Value in parentheses is the free R_{cryst} determined from 5% of the data.

FGF-R1. As a result, the aminosulfonyl or carboxylic acid group in **4c** and **4d**, respectively, may be able to form better hydrogen-bond contacts with the side chain of Asn391 and the peptide backbone of Asp404 in p60^{c-Src} when compared to FGF-R1. However, these hydrophilic substituents appeared to have less impact on the inhibitory activity against PDGF-Rβ. In contrast to this latter finding, lipophilic substituents at the C-6 position of the **4a** series (**4e–i**), in general, greatly decreased or abolished the inhibitory potencies against all kinases analyzed in this study. Compound **4e**, containing a methoxy substituent at the C-6 position, was the exception to this and inhibited PDGF-Rβ kinase with an IC₅₀ value of 3.46 μM. Additionally, this series of compounds was found to be inactive toward EGF-R tyrosine kinase.

The kinase inhibitory activities of these inhibitors generally translated well into inhibition of growth factor-dependent cell proliferation. In this regard, compounds **4a–d** were found to show preferential inhibition of VEGF-dependent HUVEC proliferation when compared to their inhibitory activities against FGF-, PDGF-, and EGF-dependent cell proliferation. In contrast, poor kinase inhibitors such as compounds **4e–i** containing the lipophilic substituents at the C-6 position of the

indolin-2-one core, in general, showed low inhibitory activity or were inactive in the cell proliferation assays. However, it is worth noting that **4e** inhibited the PDGF-R tyrosine kinase in both the kinase and cell-based assays. Of particular interest, compound **4c** inhibited EGF-induced cell proliferation (IC₅₀ = 6.0 μM), even though it was found to be inactive toward EGF-R kinase. This might be, in part, due to its potent inhibitory activity against the p60^{c-Src} kinase that has been shown to be required for EGF-dependent signal transduction pathway.¹³ It is of interest that compound **4e** was found to be 4-fold more potent than **4h** against the PDGF-R tyrosine kinase but of equal potency as **4h** toward PDGF-dependent cell proliferation. Furthermore, **4b** was over 10-fold more potent than **4c** in the PDGF-R kinase assay but 8-fold less potent in the PDGF-stimulated cell growth assay. This could be due to other factors, including the ability of the inhibitor to penetrate cell membranes or the chemical stability of the compound in cells, and might also affect the outcome of signal transduction events following receptor activation. Compound **4d** (Table 1) of this series was the most potent inhibitor of the three targets with regard to inhibiting both kinases and growth factor-dependent proliferation.

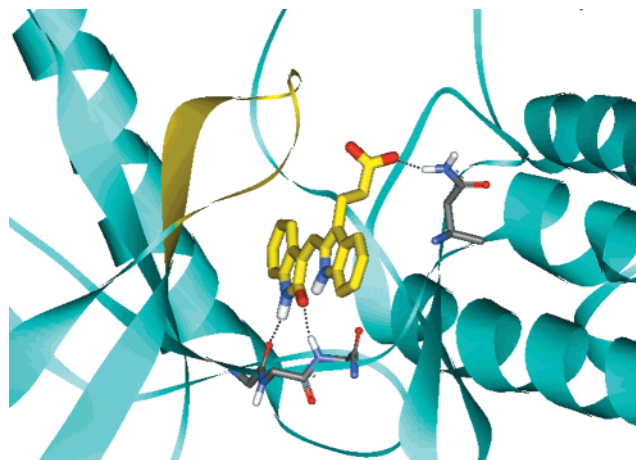


Figure 1. Crystallographic analysis of compound **9a** in the ATP-binding pocket of FGF-R1 tyrosine kinase. Hydrogen bonds are shown between compound **9a** and FGF-R1 (dotted lines). The nucleotide-binding loop is colored yellow for visualization and has undergone a conformational change relative to crystallographic analysis of FGF-R1 in the absence of **9a**.

B. Substituted 3-[2-(2-Oxo-1,2-dihydroindol-3-ylidenemethyl)-4,5,6,7-tetrahydro-1*H*-indol-3-yl]-propionic Acids. Previously, we have shown that the propionic acid functionality at the C-3' position of the pyrrole ring could enhance the inhibitory activity against both VEGF-R2 (Flk-1) and FGF-R1.^{9,12} Therefore, in this study, we prepared the **9a** series (Table 2) in order to improve the inhibitory activities against the VEGF-R2 (Flk-1) and FGF-R1 kinases. Additionally, we have cocrystallized the prototype compound, **9a**, within the catalytic domain of the FGF-R1 tyrosine kinase in order to guide our understanding of the molecular mechanism for this type of indolin-2-one series and to direct further structural modification (Figure 1). Cocrystallographic methods, X-ray diffraction, and refinement were similar to that described previously¹² and are more specifically described in the Experimental Section (Table 3).

The crystallographic structure of **9a** within the catalytic domain of the FGF-R1 kinase revealed that **9a** binds to the receptor in a manner similar to that of compound **2** (Table 2) described previously.¹² The indolin-2-one core of compound **9a** was found to occupy the adenine-binding site of FGF-R1 through a bidentate hydrogen-bond donor–acceptor system. In this case, the NH-1 and C=O of the indolin-2-one core were found to form hydrogen bonds to the two backbone amino acid residues, Glu562 and Ala564, in the hinge region of the FGF-R1 catalytic domain. The tetrahydroindole moiety of **9a** projected to the opening of the ATP-binding cleft. The NH-1' of the tetrahydroindole ring was found to form an intramolecular hydrogen bond to the carbonyl oxygen at the C-2 position of the indolin-2-one core. In addition, a conformational change in the nucleotide-binding loop was found to occur in a manner similar to that observed previously in the **2**–FGF-R1 cocrystal structure due to an interaction between the propionic acid moiety at the C-3' position of the tetrahydroindole side chain and Asn568 in the hinge region. It is also worth noting that three methylene moieties of the tetrahydroindole ring were found to be exposed to the solvent.

It is of interest to interpret the biological activities of compound **9a** in context of the crystallographic informa-

tion. The prototype compound **9a** (Table 2) was found to be 5-, 39-, and 23-fold more potent than **4a** (Table 1) toward VEGF-R2 (Flk-1), FGF-R1, and PDGF-R β kinases, respectively. Given the crystallographic information, the increased potencies may be due to favorable interactions of the propionic acid functionality of **9a** with Asn568 within the catalytic domains of VEGF-R2 (Flk-1/KDR) or FGF-R1 kinase and the aspartic acid or aspartate of PDGF-R β .¹² A comparison of compound **9a** to **2** indicated that compound **9a** was 5- and 9-fold less potent toward VEGF-R2 (Flk-1) and FGF-R1 kinases, respectively, and showed similar inhibitory activity toward the PDGF-R β kinase. This might be the result of the unfavorable interactions of the lipophilic cyclohexyl ring of tetrahydroindole within the hydrophilic environment at the opening of the ATP-binding site of VEGF-R2 (Flk-1/KDR) and FGF-R1 kinases. Interestingly, **9a** was found to be 5-fold more potent than **2** when tested against p60^{c-Src} kinase. In this regard, it is in accordance with the results from the **4a** series (**4a** compared to **1** in Table 1) which suggested that the tetrahydroindole-containing indolin-2-ones might favor p60^{c-Src} inhibition when compared to the corresponding pyrrole-containing analogues.

SAR analysis of a bromo substitution at the C-5 position of the **9b** was found to improve the inhibitory activity against both VEGF-R2 (Flk-1) (IC₅₀ = 0.03 μ M) and PDGF-R β (IC₅₀ = 0.004 μ M) kinases and retained the potent inhibitory activities against FGF-R1 (IC₅₀ = 0.27 μ M) and p60^{c-Src} (IC₅₀ = 1.27 μ M) kinases when compared to **9a** (Table 2). Compound **9b** represented the most potent inhibitor of PDGF-R β tyrosine kinase in this report. The same SAR trend was observed for **4a** series (Table 1) where bromination at the C-5 position of the **4a** resulted in the most potent PDGF-R inhibitor (compound **4b**) of the series.

According to our previous study,⁹ hydrophilic substitution at the C-5 position of the indolin-2-one core (e.g. aminosulfonyl or carboxylic acid) was found to increase the inhibitory potency of indolin-2-ones toward both VEGF-R2 (Flk-1) and FGF-R1. Thus, in this study, these same hydrophilic substituents were also introduced into the core of **9a**. Unlike our previous series, a hydrophilic aminosulfonyl moiety at the C-5 position of **9c** decreased the potency toward VEGF-R2 (Flk-1) and retained the inhibitory activity against both FGF-R1 and PDGF-R kinases. On the other hand, compound **9d**, containing a carboxylic acid moiety at the C-5 position of the core, was found to be 22- and 12-fold more potent than **9a** toward VEGF-R2 (Flk-1) and PDGF-R β kinases, respectively. This SAR was found to be different from that deduced from our own previous study where analogues containing the propionic acid group at the C-4' position of the pyrrole ring tended to increase the inhibitory potencies toward both VEGF-R2 and FGF-R1 kinases and retained or decreased activity against the PDGF-R kinase.⁹ This discrepancy could be the result of different receptor binding modes for the two series. In this regard, the receptor conformational change has been observed within the **9a**–FGF-R1 cocrystal structure whereas such change has not been found in the cocrystal structure of FGF-R1 and the compound with a propionic acid at the C-4' position of the pyrrole ring.¹¹ In addition, both **9c** and **9d** were found to be more potent than **9a**

when tested toward p60^{c-Src} kinase. This is in accordance with the SAR of the **4a** series where the hydrophilic substituents greatly enhanced the p60^{c-Src} kinase inhibitory activity (compounds **4c** and **4d** compared to **4a**). Phenyl or substituted phenyl substituents at the C-6 position on the **9a** core, in general, were found to increase the inhibitory potencies toward p60^{c-Src} kinase, retain the inhibitory activity against VEGF-R2 (Flk-1), and decrease the potency toward FGF-R1 and PDGF-R kinases. Two exceptions to this general observation were compounds **9f** and **9h**, which were more potent than **9a** when tested against PDGF-R β (**9f**: IC₅₀ = 0.04 μ M) and FGF-R1 (**9h**: IC₅₀ = 0.08 μ M) kinases, respectively (Table 2). In addition, most of these **9a** analogues were found to be inactive against the EGF-R tyrosine kinase.

In the cell proliferation assays, most of the compounds in the **9a** series were found to inhibit VEGF-, FGF-, and PDGF-dependent cell proliferations with some compounds with more selectivity toward inhibition of VEGF-dependent HUVEC proliferation (Table 2). Specifically, compounds **9a** and **9b** inhibited VEGF-dependent HUVEC proliferation with IC₅₀ values of 2 and 0.3 nM, respectively. Both compounds were also found to be good inhibitors of FGF-dependent HUVEC proliferation with IC₅₀ values of 10 and 100 nM, respectively. However, compound **9b**, the most potent PDGF-R β kinase inhibitor (IC₅₀ = 4 nM), inhibited PDGF-dependent cell proliferation with an IC₅₀ value of 1.38 μ M. The lack of concordance between the two types of assays for the highly polar compounds **9c** and **9d** might be due to poor cell membrane permeability as discussed in our previous report.⁹ Other factors might help explain this discordance including chemical stability, solubility, or binding to serum proteins in the tissue culture media. In general, the **9a** series was found to be more potent than the **4a** series to block cell proliferations.

Conclusions

In this study, we have explored a new indolin-2-one pharmacophore that contains the tetrahydroindole moiety at the C-3 position of the indolin-2-one core in order to determine potency and selectivity of these compounds to inhibit VEGF-R2 (Flk-1/KDR), FGF-R1, and PDGF-R β tyrosine kinases. In this regard, these compounds were evaluated for their relative inhibitory activity against a broad panel of tyrosine kinases and growth factor-mediated signal transduction in cells.

The relationships between compounds in regard to the inhibitory activities of VEGF-R2 (Flk-1), FGF-R1, PDGF-R β , p60^{c-Src}, and EGF-R tyrosine kinases were interpreted in the context of crystallographic analysis of **9a**–FGF-R1 and protein structural models. First, it appears that the propionic acid moiety is required for high potencies against all three target RTKs (**9a** series compared to **4a** series). Second, acidic substituents (i.e. aminosulfonyl or carboxyl group) at the C-5 position of the **4a** series resulted in favorable inhibitory activities against both VEGF-R2 (Flk-1) and FGF-R1 (i.e. **4c** and **4d** compared to **4a**). In contrast, the hydrophilic substituent at the C-5 position of the **9a** series resulted in different effects on the inhibitory activity against these kinases (**9c** and **9d** compared to **9a**). This difference might be the result of different binding modes for **9a**

and **4a** that may be due to the presence or absence of conformational changes upon binding. Third, the aryl substituents at the C-6 position of the **4a** core tended to decrease, if not abolish, the potency against all three targets including p60^{c-Src} kinase. On the other hand, aryl substituents in **9a**-related compounds retained inhibitory potencies toward VEGF-R2 (Flk-1) and PDGF-R β kinases, decreased inhibitory activity against FGF-R1 kinase, and increased activity when tested against p60^{c-Src} kinase. Finally, all of the compounds in this study were found to be inactive against the EGF-R tyrosine kinase.

To date, the indolin-2-one series described in this report exhibits the most profound potencies to block growth factor-mediated signal transduction as measured by cell proliferation. In this regard, these compounds were found to inhibit signaling due to stimulation of VEGF, FGF, and PDGF receptors in contrast to the EGF receptor. We have extended this selectivity to show that these compounds have no effect to block cell proliferation following stimulation of the IGF-1 receptor as well (data not shown). We conclude, therefore, that these compounds are relatively specific to inhibition of "split" tyrosine kinases. In contrast, the activities of these compounds on the p60^{c-Src} kinases would not have been explained purely on the receptor architecture since the p60^{c-Src} kinase is a cytoplasmic tyrosine kinase without a kinase insert domain. Nonetheless, models of p60^{c-Src} kinase have been constructed and, in the vicinity of the adenine-binding pocket, help explain the potencies of these compounds to inhibit this enzyme.

In summary, we have prepared compounds that can inhibit VEGF-R2 (Flk-1/KDR), FGF-R1, and PDGF-R β tyrosine kinases. Since all three RTKs play crucial roles in tumor growth and the tumor angiogenic process, a single compound with this type of target profile may be advantageous as a therapeutic. Further in vivo studies of those compounds may be useful to test for the treatment of angiogenesis-related diseases, such as cancer, diabetic retinopathies, atherosclerosis, psoriasis, and rheumatoid arthritis. In addition, these compounds may have utility in the treatment of PDGF and FGF growth factor-related disorders, including cancer and tissue injury, where these receptor systems have been implicated.

Experimental Section

NMR spectra were recorded by Acorn NMR using a Nicolet NT300 or Nicolet NT360. Tetramethylsilane (TMS) was used as an internal standard and chemical shifts are reported in parts per million (δ) downfield from TMS. Coupling constants are reported in hertz (Hz). Mass spectra (electron spray) were recorded by SYNPEP Corp., using an API I PLUS spectrometer. Elemental analyses were performed by Galbraith Laboratories, Inc. Elemental analysis results are within $\pm 0.4\%$ of the theoretical values.

3-(4,5,6,7-Tetrahydro-1H-indol-2-ylmethylene)-1,3-dihydroindol-2-one (4a). Dimethylformamide (2.2 mL, 28.5 mmol) and 240 mL of dichloromethane were cooled to -4°C in an ice-salt bath maintained at -10°C . Phosphorus oxychloride (2.7 mL, 28.5 mmol) was rapidly added via the dropping funnel. The reaction mixture was further stirred at room temperature for 30 min and then cooled to 0°C . 4,5,6,7-Tetrahydro-1H-indole (2.3 g, 19 mmol) was added portionwise to the above reaction mixture. The mixture was refluxed for 1 h, cooled to 5°C , diluted with 2 N potassium hydroxide to pH 10, and further stirred at room temperature for 1 h. The

precipitate was filtered, washed with water and dried to give 2.0 g (70% yield) of 4,5,6,7-tetrahydro-1*H*-indole-2-carbaldehyde (**3**) as a tan solid: ¹H NMR (360 MHz, DMSO-*d*₆) δ 11.56 (s, br, 1H, NH-1), 9.26 (s, 1H, CHO-2), 6.66 (d, *J* = 2.12 Hz, 1H, H-3'), 2.54 (t, *J* = 6.18 Hz, 2H, CH₂CH₂CH₂CH₂), 2.43 (t, *J* = 5.88 Hz, 2H, CH₂CH₂CH₂CH₂), 1.62–1.75 (m, 4H, CH₂CH₂CH₂CH₂); MS *m/z* (relative intensity, %) 150 ([M + 1]⁺, 100).

A mixture of **3** (90 mg, 0.60 mmol), 67 mg (0.50 mmol) of oxindole and 1 drop of piperidine in 2 mL of ethanol was heated to 95 °C overnight. The reaction mixture was cooled and precipitate was filtered, washed with cold ethanol and hexane, and dried in a vacuum oven overnight to give 121 mg (92%) of 6-(3-methoxy-phenyl)-3-(4,5,6,7-tetrahydro-1*H*-indol-2-ylmethylene)-1,3-dihydroindol-2-one as a brown solid: ¹H NMR (300 MHz, DMSO-*d*₆) δ 13.13 (s, 1H, NH-1'), 10.79 (s, br, 1H, NH-1), 7.59 (s, 1H, H-vinyl), 7.58 (d, *J* = 7.95 Hz, 1H, H-4), 7.10 (t, *J* = 7.95 Hz, 1H, H-6), 6.97 (t, *J* = 7.95 Hz, 1H, H-5), 6.87 (d, *J* = 7.95 Hz, 1H, H-7), 6.59 (s, br, 1H, H-3'), 2.71 (t, *J* = 5.92 Hz, 2H, CH₂CH₂CH₂CH₂), 2.52 (t, *J* = 3.33 Hz, 2H, CH₂CH₂CH₂CH₂), 1.70–1.80 (m, 4H, CH₂CH₂CH₂CH₂). Anal. (C₁₇H₁₆N₂O) C, H, N.

5-Bromo-3-(4,5,6,7-tetrahydro-1*H*-indol-2-ylmethylene)-1,3-dihydroindol-2-one (4b). This compound was prepared using the same method as for synthesizing **4a** with a yield of 99%: ¹H NMR (300 MHz, DMSO-*d*₆) δ 13.09 (s, 1H, NH-1'), 10.84 (s, br, 1H, NH-1'), 7.79 (d, *J* = 1.96 Hz, 1H, H-4), 7.71 (s, 1H, H-vinyl), 7.22 (dd, *J* = 1.96, 8.07 Hz, 1H, H-6), 6.80 (d, *J* = 8.07 Hz, 1H, H-7), 6.59 (s, br, 1H, H-3'), 2.71 (t, *J* = 6.12 Hz, 2H, CH₂CH₂CH₂CH₂), 2.51 (t, *J* = 6.12 Hz, 2H, CH₂CH₂CH₂CH₂), 1.68–1.79 (m, 4H, CH₂CH₂CH₂CH₂). Anal. (C₁₇H₁₅BrN₂O) C, H, N.

2-Oxo-3-(4,5,6,7-tetrahydro-1*H*-indol-2-ylmethylene)-2,3-dihydro-1*H*-indole-5-sulfonic Acid Amide (4c). This compound was prepared using the same method as for synthesizing **4a** with a yield of 79%: ¹H NMR (360 MHz, DMSO-*d*₆) δ 13.04 (s, 1H, NH-1'), 11.10 (s, 1H, NH-1), 8.01 (d, *J* = 1.72 Hz, 1H, H-4), 7.72 (s, 1H, H-vinyl), 7.57 (dd, *J* = 1.72, 8.12 Hz, 1H, H-6), 7.09 (s, br, 2H, H₂NSO₂-5), 6.99 (d, *J* = 8.12 Hz, 1H, H-7), 6.72 (s, br, 1H, H-3'), 2.72 (t, *J* = 5.64 Hz, 2H, CH₂CH₂CH₂CH₂), 2.52 (t, *J* = 5.64 Hz, 2H, CH₂CH₂CH₂CH₂), 1.70–1.79 (m, 4H, CH₂CH₂CH₂CH₂). Anal. (C₁₇H₁₇N₃O₃SC·0.25H₂O) C, H, N.

2-Oxo-3-(4,5,6,7-tetrahydro-1*H*-indol-2-ylmethylene)-2,3-dihydro-1*H*-indole-5-carboxylic Acid (4d). This compound was prepared using the same method as for synthesizing **4a** with a yield of 60%: ¹H NMR (360 MHz, DMSO-*d*₆) δ 13.00 (s, br, 1H, H-1'), 12.49 (s, vbr., 1H, COOH-5), 11.06 (s, 1H, NH-1), 8.16 (d, *J* = 1.60 Hz, 1H, H-4), 7.77 (s, 1H, H-vinyl), 7.74 (dd, *J* = 1.81, 8.28 Hz, 1H, H-6), 6.94 (d, *J* = 8.28 Hz, 1H, H-7), 6.66 (s, br, 1H, H-3'), 2.71 (t, *J* = 5.85 Hz, 2H, CH₂CH₂CH₂CH₂), 2.52 (t, *J* = 6.00 Hz, 2H, CH₂CH₂CH₂CH₂), 1.70–1.79 (m, 4H, CH₂CH₂CH₂CH₂). Anal. (C₁₈H₁₆N₂O₃·0.5H₂O) C, H, N.

6-Methoxy-3-(4,5,6,7-tetrahydro-1*H*-indol-2-ylmethylene)-1,3-dihydroindol-2-one (4e). This compound was prepared using the same method as for synthesizing **4a** with a yield of 90%: ¹H NMR (300 MHz, DMSO-*d*₆) δ 12.90 (s, br, 1H, NH-1'), 10.72 (s, 1H, NH-1), 7.46 (d, *J* = 8.44 Hz, 1H, H-4), 7.42 (s, 1H, H-vinyl), 6.55 (dd, *J* = 2.16, 8.44 Hz, 1H, H-5), 6.49 (d, *J* = 1.78 Hz, 1H, H-3'), 6.43 (d, *J* = 2.16 Hz, 1H, H-7), 3.74 (s, 3H, OCH₃-6), 2.68 (t, *J* = 5.67 Hz, 2H, CH₂CH₂CH₂CH₂), 2.48–2.50 (m, 2H, CH₂CH₂CH₂CH₂), 1.68–1.78 (m, 4H, CH₂CH₂CH₂CH₂); MS *m/z* (relative intensity, %) 295 ([M + 1]⁺, 59). Anal. (C₁₈H₁₈N₂O₂) C, H, N.

6-Phenyl-3-(4,5,6,7-tetrahydro-1*H*-indol-2-ylmethylene)-1,3-dihydroindol-2-one (4f). This compound was prepared using the same method as for synthesizing **4a** with a yield of 70%: ¹H NMR (360 MHz, DMSO-*d*₆) δ 13.10 (s, br, 1H, NH-1'), 10.85 (s, br, 1H, NH-1), 7.61–7.66 (m, 4H, H-4, H-vinyl, and H-3',5'), 7.44 (t, br, *J* = 7.64 Hz, 2H, H-2',6'), 7.33 (t, br, *J* = 7.64, 1H, H-4'), 7.27 (dd, *J* = 1.60, 8.06 Hz, 1H, H-5), 7.10 (d, *J* = 1.60 Hz, 1H, H-7), 6.60 (s, br, 1H, H-3'), 2.71 (t, *J* = 6.02 Hz, 2H, CH₂CH₂CH₂CH₂), 2.52 (t, *J* = 6.05 Hz, 2H,

CH₂CH₂CH₂CH₂), 1.70–1.79 (m, 4H, CH₂CH₂CH₂CH₂); MS *m/z* (relative intensity, %) 341 ([M + 1]⁺, 50). Anal. (C₂₃H₂₀N₂O) C, H, N.

6-(3-Methoxyphenyl)-3-(4,5,6,7-tetrahydro-1*H*-indol-2-ylmethylene)-1,3-dihydroindol-2-one (4g). This compound was prepared using the same method as for synthesizing **4a** with a yield of 92%: ¹H NMR (360 MHz, DMSO-*d*₆) δ 13.10 (s, br, 1H, NH-1'), 10.83 (s, br, 1H, NH-1), 7.64 (d, *J* = 7.95 Hz, 1H, H-4), 7.62 (s, 1H, H-vinyl), 7.35 (t, *J* = 7.95 Hz, 1H, H-5'), 7.28 (dd, *J* = 1.58, 7.95 Hz, 1H, H-5), 7.19 (d, *J* = 7.95 Hz, 1H, H-4'), 7.13 (t, *J* = 2.25 Hz, 1H, H-2'), 7.09 (d, *J* = 1.58 Hz, 1H, H-7), 6.90 (dd, *J* = 2.25, 7.95 Hz, 1H, H-6'), 6.60 (s, br, 1H, H-3'), 3.82 (s, 3H, OCH₃-3'), 2.71 (t, *J* = 6.00 Hz, 2H, CH₂CH₂CH₂CH₂), 2.52 (t, *J* = 6.11 Hz, 2H, CH₂CH₂CH₂CH₂), 1.70–1.79 (m, 4H, CH₂CH₂CH₂CH₂); MS *m/z* (relative intensity, %) 371 ([M + 1]⁺, 100). Anal. (C₂₄H₂₂N₂O₂) C, H, N.

6-(2-Methoxyphenyl)-3-(4,5,6,7-tetrahydro-1*H*-indol-2-ylmethylene)-1,3-dihydroindol-2-one (4h). This compound was prepared using the same method as for synthesizing **4a** with a yield of 85%: ¹H NMR (360 MHz, DMSO-*d*₆) δ 13.11 (s, br, 1H, NH-1'), 10.74 (s, br, 1H, NH-1'), 7.58 (d, *J* = 7.41 Hz, 1H, H-4), 7.58 (s, 1H, H-vinyl), 7.27–7.34 (m, 2H), 6.99–7.10 (m, 4H), 6.58 (s, br, 1H, H-3'), 3.76 (s, 3H, OCH₃-2'), 2.71 (t, *J* = 5.91 Hz, 2H, CH₂CH₂CH₂CH₂), 2.52 (t, *J* = 6.01 Hz, 2H, CH₂CH₂CH₂CH₂), 1.7–1.79 (m, 4H, CH₂CH₂CH₂CH₂); MS *m/z* (relative intensity, %) 371 ([M + 1]⁺, 100). Anal. (C₂₄H₂₂N₂O₂) C, H, N.

6-(4-Methoxyphenyl)-3-(4,5,6,7-tetrahydro-1*H*-indol-2-ylmethylene)-1,3-dihydroindol-2-one (4i). This compound was prepared using the same method as for synthesizing **4a** with a yield of 50%: ¹H NMR (360 MHz, DMSO-*d*₆) δ 13.07 (s, br, 1H, NH-1'), 10.80 (s, br, 1H, NH-1), 7.61 (d, *J* = 8.02 Hz, 1H, H-4), 7.58 (s, 1H, H-vinyl), 7.56 (d, *J* = 8.83 Hz, 2H, H-3',5'), 7.21 (dd, *J* = 1.57, 8.02 Hz, 1H, H-5), 7.04 (d, *J* = 1.57 Hz, 1H, H-7), 7.00 (d, *J* = 8.83 Hz, 2H, H-2',6'), 6.58 (d, br, *J* = 1.05 Hz, 1H, H-3'), 3.79 (s, 3H, OCH₃-4'), 2.71 (t, *J* = 6.10 Hz, 2H, CH₂CH₂CH₂CH₂), 2.51 (t, *J* = 5.96 Hz, 2H, CH₂CH₂CH₂CH₂), 1.70–1.79 (m, 4H, CH₂CH₂CH₂CH₂); MS *m/z* (relative intensity, %) 371 ([M + 1]⁺, 100). Anal. (C₂₄H₂₂N₂O₂) C, H, N.

3-[2-(2-Oxo-1,2-dihydroindol-3-ylidenemethyl)-4,5,6,7-tetrahydro-1*H*-indol-3-yl]propionic Acid (9a). 1-(Morpholin-4-yl)cyclohexene (20.1 g, 120 mmol), 14.4 g (142 mmol) of triethylamine and 100 mL of dichloromethane were charged to a 1-L, three-neck round-bottom flask equipped with a reflux condenser, mechanical stirring, a thermometer and a dropping funnel. The mixture was refluxed for 15 min and cooled in a water bath to 15–20 °C. With vigorous stirring 18 g (109 mmol) of ethylsuccinyl chloride dissolved in 40 mL of dichloromethane was added over 5 min via the dropping funnel. At the end of the addition the mixture contained a large amount of precipitate and was refluxing. Refluxing was continued for 30 min and the mixture was cooled to ambient temperature in a water bath. The mixture was extracted twice with 100 mL of water each time and twice with 30 mL of brine each time, dried over 5 g of anhydrous sodium sulfate and evaporated to give crude 4-(2-morpholin-4-ylcyclohex-1-enyl)-4-oxobutyric acid ethyl ester (**5**) as an oil.

Crude **5** (30 g, 102 mmol), 26.7 g (126 mmol) of diethyl aminomalonate hydrochloride, 10.8 g (132 mmol) of sodium acetate and 28 mL of glacial acetic acid were charged to a 1-L, three-neck round-bottom flask equipped with mechanical stirring, a reflux condenser and heated in an oil bath. The mixture was heated to 108 °C over 30 min accompanied by the evolution of carbon dioxide and the formation of a precipitate of sodium chloride. The mixture was held at 100–108 °C for 2 h and cooled to about 50 °C in a water bath. Water (160 mL) and 160 mL of ethyl acetate were added. The precipitate dissolved. The ethyl acetate layer was separated and washed twice with 100 mL of water each time, once with 70 mL of saturated sodium bicarbonate solution, once with 50 mL of brine, dried over 10 g of anhydrous sodium sulfate and rotary evaporated to give 30 g (85% yield) of crude 2-ethoxy-

carbonyl-3-(2-ethoxycarbonyl)ethyl)-4,5,6,7-tetrahydroindole (**6**) as an oil: $^1\text{H NMR}$ (400 MHz, $\text{DMSO}-d_6$) δ 11.09 (s, 1H, NH-1), 4.18 (q, $J = 6.9$ Hz, 2H, $\text{COOCH}_2\text{CH}_3$), 4.03 (q, $J = 7.2$ Hz, 2H, $\text{CH}_2\text{CH}_2\text{COOCH}_2\text{CH}_3$), 2.84 (t, $J = 8.0$ Hz, 2H, $\text{CH}_2\text{CH}_2\text{COOCH}_2\text{CH}_3$), 2.49 (t, $J = 5.4$ Hz, 2H, $\text{CH}_2\text{CH}_2\text{CH}_2\text{CH}_2$), 2.42 (t, $J = 8.0$ Hz, 2H, $\text{CH}_2\text{CH}_2\text{COOCH}_2\text{CH}_3$), 2.34 (t, $J = 5.4$ Hz, 2H, $\text{CH}_2\text{CH}_2\text{CH}_2\text{CH}_2$), 1.66 (t, $J = 5.4$ Hz, 4H, $\text{CH}_2\text{CH}_2\text{CH}_2\text{CH}_2$), 1.26 (t, $J = 6.9$ Hz, 3H, $\text{COOCH}_2\text{CH}_3$), 1.16 (t, $J = 7.2$ Hz, 3H, $\text{COOCH}_2\text{CH}_3$).

Crude **6** (30 g, 102 mmol) and 80 mL (400 mmol) of 5 N sodium hydroxide were refluxed for 80 min in a round-bottom flask heated in an oil bath and equipped with magnetic stirring. The heater was turned off but the flask left in the hot bath and about 44 mL (440 mmol) of 10 N hydrochloric acid was cautiously added via a dropping funnel through the reflux condenser with vigorous stirring. When approximately 80% of the acid had been added, a large amount of carbon dioxide was evolved. The addition was continued until the pH was 2–3. The mixture was cooled in a water bath and 200 mL of ethyl acetate was added to dissolve the oil that was present. The ethyl acetate layer was isolated, washed 3 times with 50 mL of water each time and twice with 30 mL of brine each time, dried over 5 g of anhydrous sodium sulfate and evaporated to give 15.5 g (80%) yield of crude 3-(2-carboxyethyl)-4,5,6,7-tetrahydroindole (**7**) as a very dark sticky syrup: $^1\text{H NMR}$ (400 MHz, $\text{DMSO}-d_6$) δ 12.0 (s, 1H COOH), 9.92 (br, 1H, NH-1), 6.26 (d, $J = 1.6$ Hz, 1H, H-2), 2.28–2.51 (m, 8H, $\text{CH}_2 \times 4$), 1.64–1.78 (m, 4H, $\text{CH}_2 \times 2$).

Dimethylformamide (11.7 g, 160 mmol) and 240 mL of dichloromethane in a 1-L, three-neck round-bottom flask equipped with magnetic stirring, a reflux condenser and a dropping funnel were cooled to -4 °C in an ice–salt bath maintained at -10 °C. Phosphorus oxychloride (24.5 g, 160 mmol) was rapidly added via the dropping funnel. The temperature increased to -3 °C and then, with further stirring, decreased to -7 °C. Crude **7** (15.5 g, 80 mmol) dissolved in 160 mL of dichloromethane was added via the dropping funnel over 15 min keeping the temperature below 1 °C. The mixture was refluxed for 10 min, cooled to 5 °C, and diluted with 300 mL of water. The aqueous layer was evaporated and saved and the organic layer extracted with another 30 mL of water. The aqueous layers were combined, washed with 30 mL of dichloromethane and cooled to 5 °C. The aqueous layer was adjusted to pH 10 with about 48 mL of 10 N sodium hydroxide accompanied by a temperature increase to 15 °C. The mixture was then cooled to 10 °C and adjusted to pH 2–3 with about 48 mL of 10 N hydrochloric acid. The oil which formed solidified and was collected by vacuum filtration, washed three times with 20 mL of water each time and dried under high vacuum to give 5.5 g (31% yield) of 3-(2-formyl-4,5,6,7-tetrahydro-1*H*-indol-3-yl)propionic acid (**8**) as a brown solid: $^1\text{H NMR}$ (360 MHz, $\text{DMSO}-d_6$) δ 11.4 (s, 1H, NH-1), 9.24 (s, 1H, CHO-2), 2.80 (t, $J = 9.2$ Hz, 2H, $\text{CH}_2\text{CH}_2\text{COOH}$), 2.35–2.50 (m, 6H, $\text{CH}_2 \times 3$), 1.64–1.89 (m, 4H, $\text{CH}_2 \times 2$).

Compound **8** (5.4 g, 24 mmol), 3.57 g (27 mmol) of indolin-2-one and 25 mL of ethanol were heated to near reflux in a 250-mL, three-neck round-bottom flask equipped with a reflux condenser and mechanical stirring. Piperidine (2.7 g, 310 mmol) was slowly added and the mixture refluxed for 4 h. Acetic acid (8 mL) was slowly added causing a voluminous precipitate. The mixture was refluxed for 5 min and cooled to ambient temperature. The precipitate was collected by vacuum filtration and washed with 20 mL of ethanol. The solids were slurry-washed by refluxing in 30 mL of ethanol, cooled, collected by vacuum filtration, washed with 30 mL of ethanol and dried under high vacuum to give 5.5 g (68% yield) of 3-[2-(2-oxo-1,2-dihydroindol-3-ylidene)ethyl]-4,5,6,7-tetrahydro-1*H*-indol-3-yl]propionic acid (**9a**) as an orange solid: $^1\text{H NMR}$ (360 MHz, $\text{DMSO}-d_6$) δ 13.27 (s, 1H, NH-1'), 12.09 (s, br, 1H, $\text{CH}_2\text{CH}_2\text{COOH-3'}$), 10.71 (s, 1H, NH-1), 7.65 (d, $J = 7.52$ Hz, 1H, H-4) 7.60 (s, 1H, H-vinyl), 7.07 (dt, $J = 1.05, 7.52$ Hz, 1H, H-5), 6.95 (dt, $J = 1.05, 7.52$ Hz, 1H, H-6), 6.85 (d, $J = 7.52$ Hz, 1H, H-7), 2.90 (t, $J = 7.65$ Hz, 2H, $\text{CH}_2\text{CH}_2\text{COOH-3'}$), 2.66 (t, $J = 5.59$ Hz, 2H, $\text{CH}_2\text{CH}_2\text{CH}_2\text{CH}_2$), 2.39–2.47 (m, 4H,

$\text{CH}_2\text{CH}_2\text{COOH-3'}$, $\text{CH}_2\text{CH}_2\text{CH}_2\text{CH}_2$), 1.70–1.77 (m, 4H, $\text{CH}_2\text{CH}_2\text{CH}_2\text{CH}_2$). Anal. ($\text{C}_{20}\text{H}_{20}\text{N}_2\text{O}_3$) C, H, N.

3-[2-(5-Bromo-2-oxo-1,2-dihydroindol-3-ylidene)ethyl]-4,5,6,7-tetrahydro-1*H*-indol-3-yl]propionic Acid (9b**)**. Compound **8** (15.9 g, 72 mmol), 12.7 g (60 mmol) of 5-bromo-2-indolin-2-one and 150 mL of ethanol were heated to near reflux in a 500-mL, three-neck round-bottom flask equipped with a reflux condenser and magnetic stirring. Piperidine (6.4 g, 76 mmol) was slowly added and the mixture refluxed for 1 h at which time a large amount of reddish precipitate was present. Thin-layer chromatography (silica gel, ethyl acetate) showed no starting materials remaining. Acetic acid (20 mL) was slowly added causing a voluminous precipitate. The mixture was refluxed for 5 min and cooled to ambient temperature. The precipitate was collected by vacuum filtration and washed with 30 mL of ethanol. The solids were slurry-washed by refluxing in 40 mL of ethanol, cooled, collected by vacuum filtration, washed with 30 mL of ethanol and dried under high vacuum to give 22.3 g (89% yield) of 3-[2-(5-bromo-2-oxo-1,2-dihydroindol-3-ylidene)ethyl]-4,5,6,7-tetrahydro-1*H*-indol-3-yl]propionic acid (**9b**) as a red-orange solid: $^1\text{H NMR}$ (360 MHz, $\text{DMSO}-d_6$) δ 13.32 (s, 1H, NH-1'), 12.12 (s, br, 1H, $\text{CH}_2\text{CH}_2\text{COOH-3'}$), 10.86 (s, 1H, NH-1), 7.96 (d, $J = 1.91$ Hz, 1H, H-4) 7.71 (s, 1H, H-vinyl), 7.19 (dd, $J = 1.91, 8.19$ Hz, 1H, H-6), 6.79 (d, $J = 8.19$ Hz, 1H, H-7), 2.92 (t, $J = 7.55$ Hz, 2H, $\text{CH}_2\text{CH}_2\text{COOH-3'}$), 2.66 (t, $J = 5.25$ Hz, 2H, $\text{CH}_2\text{CH}_2\text{CH}_2\text{CH}_2$), 2.40–2.44 (m, 4H, $\text{CH}_2\text{CH}_2\text{COOH-3'}$, $\text{CH}_2\text{CH}_2\text{CH}_2\text{CH}_2$), 1.70–1.77 (m, 4H, $\text{CH}_2\text{CH}_2\text{CH}_2\text{CH}_2$). Anal. ($\text{C}_{20}\text{H}_{19}\text{BrN}_2\text{O}_3$) C, H, N.

3-[2-(2-Oxo-5-sulfamoyl-1,2-dihydroindol-3-ylidene)ethyl]-4,5,6,7-tetrahydro-1*H*-indol-3-yl]propionic Acid (9c**)**. This compound was prepared using the same procedure as for preparation of **9b** with a yield of 60%: $^1\text{H NMR}$ (300 MHz, $\text{DMSO}-d_6$) δ 13.33 (s, br, 1H, NH-1'), 12.15 (s, br, 1H, $\text{CH}_2\text{CH}_2\text{COOH-3'}$), 11.12 (s, 1H, NH-1), 8.11 (s, 1H, H-vinyl), 7.71 (s, 1H, H-4), 7.55 (d, $J = 8.26$ Hz, 1H, H-6), 7.13 (s, br, 2H, SO_2NH_2), 6.98 (d, $J = 8.26$ Hz, 1H, H-7), 2.93 (t, $J = 6.92$ Hz, 2H, $\text{CH}_2\text{CH}_2\text{COOH-3'}$), 2.69 (s, br, $\text{CH}_2\text{CH}_2\text{CH}_2\text{CH}_2$), 2.41–2.48 (m, 4H, $\text{CH}_2\text{CH}_2\text{COOH-3'}$ and $\text{CH}_2\text{CH}_2\text{CH}_2\text{CH}_2$), 1.61–1.73 (m, 4H, $\text{CH}_2\text{CH}_2\text{CH}_2\text{CH}_2$); MS m/z (relative intensity, %) 415 (M^+ , 100). Anal. ($\text{C}_{20}\text{H}_{21}\text{N}_3\text{O}_5\text{S} \cdot 1.25\text{H}_2\text{O}$) C, H, N.

3-[3-(2-Carboxyethyl)-4,5,6,7-tetrahydro-1*H*-indol-2-ylmethylene]-2-oxo-2,3-dihydro-1*H*-indole-5-carboxylic Acid (9d**)**. This compound was prepared using the same procedure as for preparation of **9b** with a yield of 13%: $^1\text{H NMR}$ (300 MHz, $\text{DMSO}-d_6$) δ 13.27 (s, br, 1H, NH-1'), 12.34 (s, br, 2H, $\text{CH}_2\text{CH}_2\text{COOH-3'}$ and COOH-5), 11.08 (s, 1H, NH-1), 8.27 (s, 1H, H-vinyl), 7.76 (s, 1H, H-4), 7.72 (d, $J = 8.05$ Hz, 1H, H-6), 6.93 (d, $J = 8.05$ Hz, 1H, H-7), 2.94 (t, $J = 7.19$ Hz, 2H, $\text{CH}_2\text{CH}_2\text{COOH-3'}$), 2.68 (s, br, $\text{CH}_2\text{CH}_2\text{CH}_2\text{CH}_2$), 2.34–2.49 (m, 4H, $\text{CH}_2\text{CH}_2\text{COOH-3'}$ and $\text{CH}_2\text{CH}_2\text{CH}_2\text{CH}_2$), 1.64–1.73 (m, 4H, $\text{CH}_2\text{CH}_2\text{CH}_2\text{CH}_2$); MS m/z (relative intensity, %) 380 (M^+ , 100). Anal. ($\text{C}_{21}\text{H}_{20}\text{N}_2\text{O}_5 \cdot 0.25\text{H}_2\text{O}$) C, H, N.

3-[2-(6-Methoxy-2-oxo-1,2-dihydroindol-3-ylidene)ethyl]-4,5,6,7-tetrahydro-1*H*-indol-3-yl]propionic Acid (9e**)**. This compound was prepared using the same procedure as for preparation of **9b** with a yield of 50%: $^1\text{H NMR}$ (360 MHz, $\text{DMSO}-d_6$) δ 13.27 (s, br, 1H, NH-1'), 12.06 (s, vbr, 1H, $\text{CH}_2\text{CH}_2\text{COOH-3'}$), 10.80 (s, br, 1H, NH-1), 7.74 (d, $J = 7.97$ Hz, 1H, H-4), 7.64 (s, 1H, H-vinyl), 7.63 (d, $J = 7.83$ Hz, 2H, H-2'', 6''), 7.44 (t, $J = 7.83$ Hz, 2H, H-3'', 5''), 7.33 (dd, $J = 7.83$ Hz, 1H, H-4''), 7.27 (dd, $J = 1.11, 7.97$ Hz, 1H, H-5), 7.10 (d, $J = 1.11$ Hz, 1H, H-7), 2.92 (t, $J = 7.41$ Hz, 2H, $\text{CH}_2\text{CH}_2\text{COOH-3'}$), 2.67 (t, $J = 5.51$ Hz, 2H, $\text{CH}_2\text{CH}_2\text{CH}_2\text{CH}_2$), 2.41–2.46 (m, 4H, $\text{CH}_2\text{CH}_2\text{COOH-3'}$ and $\text{CH}_2\text{CH}_2\text{CH}_2\text{CH}_2$), 1.73–1.76 (m, 4H, $\text{CH}_2\text{CH}_2\text{CH}_2\text{CH}_2$); MS m/z (relative intensity, %) 411 (M^+ , 65). Anal. ($\text{C}_{26}\text{H}_{24}\text{N}_2\text{O}_3 \cdot 0.5\text{H}_2\text{O}$) C, H, N.

3-[2-(2-Oxo-6-phenyl-1,2-dihydroindol-3-ylidene)ethyl]-4,5,6,7-tetrahydro-1*H*-indol-3-yl]propionic Acid (9f**)**. This compound was prepared using the same procedure as for preparation of **9b** with a yield of 31%: $^1\text{H NMR}$ (360 MHz, $\text{DMSO}-d_6$) δ 13.27 (s, br, 1H, NH-1'), 12.06 (s, vbr, 1H, $\text{CH}_2\text{CH}_2\text{COOH-3'}$), 10.80 (s, br, 1H, NH-1), 7.74 (d, $J = 7.97$ Hz, 1H, H-4), 7.64 (s, 1H, H-vinyl), 7.63 (d, $J = 7.83$ Hz, 2H, H-2'', 6''), 7.44 (t, $J = 7.83$ Hz, 2H, H-3'', 5''), 7.33 (dd, $J = 7.83$

Hz, 1H, H-4''), 7.27 (dd, $J = 1.11, 7.97$ Hz 1H, H-5), 7.10 (d, $J = 1.11$ Hz, 1H, H-7), 2.92 (t, $J = 7.41$ Hz, 2H, $\text{CH}_2\text{CH}_2\text{COOH}$ -3'), 2.67 (t, $J = 5.51$ Hz, 2H, $\text{CH}_2\text{CH}_2\text{CH}_2\text{CH}_2$), 2.41–2.46 (m, 4H, $\text{CH}_2\text{CH}_2\text{COOH}$ -3' and $\text{CH}_2\text{CH}_2\text{CH}_2\text{CH}_2$), 1.73–1.76 (m, 4H, $\text{CH}_2\text{CH}_2\text{CH}_2\text{CH}_2$); MS m/z (relative intensity, %) 411 (M^+ , 65). Anal. ($\text{C}_{26}\text{H}_{24}\text{N}_2\text{O}_3 \cdot 0.5\text{H}_2\text{O}$) C, H, N.

3-{2-[6-(3-Methoxyphenyl)-2-oxo-1,2-dihydroindol-3-ylidenemethyl]-4,5,6,7-tetrahydro-1H-indol-3-yl}-propionic Acid (9g). This compound was prepared using the same procedure as for preparation of **9b** with a yield of 82%. ^1H NMR (360 MHz, $\text{DMSO}-d_6$) δ 13.26 (s, br, 1H, NH-1'), 10.79 (s, br, 1H, NH-1), 7.72 (d, $J = 8.09$ Hz, 1H, H-4), 7.64 (s, 1H, H-vinyl), 7.35 (t, $J = 7.94$ Hz, 1H, H-5''), 7.27 (dd, $J = 1.35, 8.09$ Hz, 1H, H-5), 7.19 (d, br, $J = 7.94$ Hz 1H, H-6''), 7.13 (t, $J = 2.02$ Hz, 1H, H-2''), 7.09 (d, $J = 1.35$ Hz, 1H, H-7), 6.90 (dd, $J = 2.02, 7.94$ Hz, 1H, H-4''), 3.80 (s, 3H, OCH_3 -3''), 2.91 (t, $J = 7.35$ Hz, 2H, $\text{CH}_2\text{CH}_2\text{COOH}$ -3'), 2.66 (t, $J = 5.88$ Hz, 2H, $\text{CH}_2\text{CH}_2\text{CH}_2\text{CH}_2$), 2.38–2.45 (m, 4H, $\text{CH}_2\text{CH}_2\text{COOH}$ -3' and $\text{CH}_2\text{CH}_2\text{CH}_2\text{CH}_2$), 1.68–1.76 (m, 4H, $\text{CH}_2\text{CH}_2\text{CH}_2\text{CH}_2$); MS m/z (relative intensity, %) 443 (M^+ , 100). Anal. ($\text{C}_{21}\text{H}_{22}\text{N}_2\text{O}_4$) C, H, N.

3-{2-[6-(2-Methoxyphenyl)-2-oxo-1,2-dihydroindol-3-ylidenemethyl]-4,5,6,7-tetrahydro-1H-indol-3-yl}-propionic Acid (9h). This compound was prepared using the same procedure as for preparation of **9b** with a yield 35%: ^1H NMR (360 MHz, $\text{DMSO}-d_6$) δ 13.26 (s, br, 1H, NH-1'), 12.06 (s, br, 1H, COOH), 10.70 (s, br, 1H, NH-1), 7.67 (d, $J = 7.72$ Hz, 1H, H-4), 7.61 (s, 1H, H-vinyl), 7.27–7.34 (m, 2H, H-4'', 5''), 7.09 (d, br, $J = 7.72$ Hz, H-6'') 7.06 (dd, $J = 1.35, 7.72$ Hz, 1H, H-5), 7.02 (dd, $J = 0.94, 7.54$ Hz, 1H, H-3''), 6.99 (d, $J = 1.35$ Hz, 1H, H-7), 3.76 (s, 3H, OCH_3 -2''), 2.91 (t, $J = 7.54$ Hz, 2H, $\text{CH}_2\text{CH}_2\text{COOH}$), 2.67 (t, $J = 5.70$ Hz, 2H, $\text{CH}_2\text{CH}_2\text{CH}_2\text{CH}_2$), 2.40–2.46 (m, 4H, $\text{CH}_2\text{CH}_2\text{COOH}$ and $\text{CH}_2\text{CH}_2\text{CH}_2\text{CH}_2$), 1.71–1.78 (m, 4H, $\text{CH}_2\text{CH}_2\text{CH}_2\text{CH}_2$); MS m/z (relative intensity, %) 441 (M^+ , 100). Anal. ($\text{C}_{27}\text{H}_{26}\text{N}_2\text{O}_4 \cdot 0.5\text{H}_2\text{O}$) C, H, N.

3-{2-[6-(4-Methoxyphenyl)-2-oxo-1,2-dihydroindol-3-ylidenemethyl]-4,5,6,7-tetrahydro-1H-indol-3-yl}-propionic Acid (9i). This compound was prepared using the same procedure as for preparation of **9b** with a yield of 30%: ^1H NMR (360 MHz, $\text{DMSO}-d_6$) δ 13.24 (s, br, 1H, NH-1), 11.61 (s, br, 1H, $\text{CH}_2\text{CH}_2\text{COOH}$ -3'), 10.76 (s, br, 1H, NH-1), 7.77 (d, $J = 8.09$ Hz, 1H, H-4), 7.61 (s, 1H, H-vinyl), 7.58 (d, $J = 8.83$ Hz, 2H, H-2'', 6'') 7.21 (dd, $J = 1.47, 8.09$ Hz, 1H, H-5), 7.04 (d, $J = 1.47$ Hz, 1H, H-7), 7.01 (d, $J = 8.83$ Hz, 2H, H-3'', 5''), 3.79 (s, 3H, OCH_3 -4''), 2.91 (t, $J = 7.35$ Hz, 2H, $\text{CH}_2\text{CH}_2\text{COOH}$ -3'), 2.67 (t, $J = 5.88$ Hz, 2H, $\text{CH}_2\text{CH}_2\text{CH}_2\text{CH}_2$), 2.40–2.47 (m, 4H, $\text{CH}_2\text{CH}_2\text{COOH}$ -3' and $\text{CH}_2\text{CH}_2\text{CH}_2\text{CH}_2$), 1.72–1.78 (m, 4H, $\text{CH}_2\text{CH}_2\text{CH}_2\text{CH}_2$); MS m/z (relative intensity, %) 441 (M^+ , 100). Anal. ($\text{C}_{27}\text{H}_{26}\text{N}_2\text{O}_4 \cdot \text{H}_2\text{O}$) C, H, N.

Cell Proliferation and Kinase Assays. These assays were described previously.⁹

X-ray Data Collection and Structure Refinement. Expression, purification and crystallization of FGF-R1 were performed as described.¹⁴ Crystals of unliganded FGF-R1 grow in space group $C2$ with two molecules in the asymmetric unit and unit cell parameters when frozen of $a = 208.9$ Å, $b = 57.5$ Å, $c = 65.7$ Å, and $\beta = 107.6$. Unliganded crystals were soaked in 500 mL of stabilizing solution [25% poly(ethylene glycol) 10000, 0.3 M $(\text{NH}_4)_2\text{SO}_4$, 0.1 M bis-Tris (pH 6.5), 5% ethylene glycol, 2% DMSO] containing 2 mM **9a** at 4 °C for 1 week. Data were collected on a Rigaku RU-200 rotating anode (Cu $K\alpha$) operating at 50 kV and 100 mA and equipped with double-focusing mirrors and an R-AXIS IIC image plate detector. Crystals were flash-cooled in a dry nitrogen stream at -175 °C. Data were processed using DENZO and SCALEPACK.¹⁵ Difference Fourier electron density maps were computed using phases calculated from the structure of unliganded FGF-R1.¹⁴

CNS was used for simulated annealing and positional/ B -factor refinement,¹⁶ and O was used for model building.¹⁷ Bulk solvent and anisotropic B -factor corrections were applied during refinement. The average B -factor is 32.5 Å² for all atoms, 32.5 Å² for protein atoms, 33.7 Å² for water molecules, and 31.4 Å² for **9a** atoms.

References

- Folkman, J. What is the evidence that tumors are angiogenesis dependent? *J. Natl. Cancer Inst.* **1990**, *82*, 4–6.
- Folkman, J.; Shing, Y. Angiogenesis. *J. Biol. Chem.* **1992**, *267*, 10931–10934.
- Strawn, L. M.; McMahon, G.; App, H.; Schreck, R.; Kuchler, W. R.; Longhi, M. P.; Hui, T. H.; Tang, C.; Levitzki, A.; Gazit, A.; Chen, I.; Keri, G.; Orfi, L.; Risau, W.; Flamme, I.; Ullrich, A.; Hirth, K. P.; Shawver, L. K. Flk-1 as a target for tumor growth inhibition. *Cancer Res.* **1996**, *56*, 3540–3545.
- Shawver, L. K.; Lipson, K. E.; Fong, T. A. T.; McMahon, G.; Plowman, G. D.; Strawn, L. M. Receptor tyrosine kinases as targets for inhibition of angiogenesis. *Drug Discovery Today* **1997**, *2* (2), 50–63.
- Pepper, M. S.; Ferrara, N.; Orci, L.; Montessano, R. Potent synergism between vascular endothelial growth factor and basic fibroblast growth factor in the induction of angiogenesis in vitro. *Biochem. Biophys. Res. Commun.* **1992**, *189*, 824–831.
- Hanahan, D.; Folkman, J. Patterns and emerging mechanisms of the angiogenic switch during tumorigenesis. *Cell* **1996**, *86*, 353–364.
- Hennequin, L. F.; Thomas, A. P.; Johnstone, C.; Ple, P.; Stokes, E. S. E.; Ogilvie, D. J.; Dukes, M.; Wedge, S. R. 90th Annual Meeting of American Association for Cancer Research, Philadelphia, PA, Apr 10–14, 1999; Abstract 457.
- Sun, L.; Tran, N.; Tang, T.; App, H.; Hirth, P.; McMahon, G.; Tang, C. Synthesis and biological evaluations of 3-substituted indolin-2-ones: a novel class of tyrosine kinase inhibitors that exhibit selectivity towards particular receptor tyrosine kinases. *J. Med. Chem.* **1998**, *41* (14), 2588–2603.
- Sun, L.; Tran, N.; Liang, C.; Tang, F.; Rice, A.; Schreck, R.; Waltz, K.; Shawver, L. K.; McMahon, G.; Tang, C. Design, synthesis, and evaluations of substituted 3-[(3- or 4-carboxyethyl)pyrrol-2-yl]methylidene]indolin-2-ones as inhibitors of VEGF, FGF, and PDGF receptor tyrosine kinases. *J. Med. Chem.* **1999**, *42* (25), 5120–5130.
- Fong, A. T. T.; Shawver, L. K.; Sun, L.; Tang, C.; App, H.; Powell, T. J.; Kim, Y. H.; Schreck, R.; Wang, X. Y.; Risau, W.; Ullrich, A.; Hirth, K. P.; McMahon, G. SU5416 is a potent and selective inhibitor of the vascular endothelial growth factor receptor (Flk-1/KDR) that inhibits tyrosine kinase catalysis, tumor vascularization, and growth of multiple tumor types. *Cancer Res.* **1999**, *59*, 99–106.
- Laird, A. D.; Vajkoczy, P.; Shawver, L. K.; Thurnher, A.; Liang, C.; Mohammadi, M.; Schlessinger, J.; Ullrich, A.; Hubbard, S. R.; Blake, R. A.; Fong, T. A. T.; Strawn, L. M.; Sun, L.; Tang, C.; Hawtin, R.; Tang, F.; Shenoy, N.; Hirth, K. P.; McMahon, G.; Cherrington, J. M. SU6668 is a potent anti-angiogenic and antitumor agent which induces regression of established tumors. *Cancer Res.*, in press.
- Mohammadi, M.; McMahon, G.; Sun, L.; Tang, P. C.; Hirth, P.; Yeh, B. K.; Hubbard, S. R.; Schlessinger, J. Structures of the tyrosine kinase domain of fibroblast growth factor receptor in complex with inhibitors. *Science* **1997**, *276*, 955–960.
- Abram, C. L.; Courtneidge, S. A. Src family tyrosine kinases and growth factor signaling. In preparation.
- Mohammadi, M.; Schlessinger, J.; Hubbard, S. R. Structure of the FGF receptor tyrosine kinase domain reveals a novel autoinhibitory mechanism. *Cell* **1996**, *86*, 577–587.
- Otwinowski, Z.; Minor, W. Processing of X-ray diffraction data collected in oscillation mode. *Methods Enzymol.* **1997**, *276*, 307–326.
- Brunger, A. T.; et al. Crystallography & NMR system: A new software suite for macromolecular structure determination. *Acta Crystallogr. D* **1998**, *54*, 905–921.
- Jones, T. A.; Zou, J. Y.; Cowan, S. W.; Kjeldgaard, M. Improved methods for building protein models in electron density maps and the location of errors in these models. *Acta Crystallogr. A* **1991**, *47*, 110–119.

JM9906116